International Journal of Thermophysics, Vol. 13, No. 1, 1992

Investigation of Si–As Solid Solutions by Pulsed Laser Heating[1]

P. Baeri,[2] R. Reitano,[2] M. A. Malvezzi,[3] and C. Sirtori[3]

Si–As supersaturated solid solutions up to 12% atomic concentration have been produced by pulsed IR laser melting of As implanted Silicon single crystal. The conditions for the solidification of a crystalline or an amorphous solution have been clarified and they have been correlated with the solidification velocity and the solid–liquid interface undercooling. Moreover, the T_0 curve, i.e., the locus of points at which the solid and the liquid phase have equal free energy, has been evaluated by remelting the solid solutions by means of pulsed UV laser irradiations. The conditions for the stability of the amorphous phase have been found.

KEY WORDS: pulsed laser heating; Si–As; solidification; solid solution.

1. INTRODUCTION

Pulsed-beam treatment of solid surfaces has two major features: fast heating, on the nanosecond or picosecond time scale, and subsequent rapid cooling and solidification. Metastable phases are often quenched-in. Conversely, a metastable phase retained at room temperature can be heated to its equilibrium temperature in the liquid phase and melted without the occurrence of any solid-phase transformation or decomposition. Pure silica has been extensively investigated. It has been shown, for example, that the transition between liquid and solid amorphous or crystalline phases of pure sililcon can be induced by nanosecond pulsed heating and there has been a considerable interest in this subject during recent years [1, 2]. The phase diagram of elemental silicon is now well established and understood.

[1] Paper presented at the Second Workshop on Subsecond Thermophysics, September 20–21, 1990, Torino, Italy.

[2] Dipartimento di Fisica, Università di Catania, Corso Italia 57, 95129 Catania, Italy.

[3] Dipartimento di Elettronica, Università di Pavia, Via Abbiategrasso 209, 27100 Pavia, Italy.

0195-928X/92/0100-0153$06.50/0

A necessary condition to observe the direct transition from the amorphous to the liquid phase is a fast heating rate ($>10^9\,\mathrm{K\cdot s^{-1}}$) in order to avoid solid-phase crystallization [3]. The transition from liquid to amorphous silicon occurs, instead, when the solidification velocity exceeds a threshold value which depends on the substrate orientation [4].

Fast solidification of binary systems is an intriguing matter since phenomena related to component partitioning, leading to interface breakdown, can occur [5]. As a starting point in the understanding of the fast solidification of binary systems, it is interesting to investigate an intermediate range of composition, i.e., the supersaturated solid solution of an element in another far from singular points, like eutectics or compound, in the relative phase diagram. We choose silicon-dopant supersaturated solution. The relationship between the thermodynamic parameters of the different phases of the solution (amorphous, crystalline, and liquid) will change continuously as a function of the solute concentration; we will thus be able to test if the picture already established for the fast solidification of pure silicon is also valid for the solution.

The metastable-phase melting temperature may in principle be determined by pulsed heating experiments, as has been done for amorphous Si [3, 6]. The melting temperature of metastable metallic alloys has already been determined by pulsed heating [7] as a function of component concentration. This technique allows the measurement of the so-called T_0 curve, i.e., the locus of temperature–concentration values where the liquid- and solid-phase free energies are equal. Since at the melting point the free energies of the liquid and the solid phase are equal, some thermodynamic parameters of the metastable phase may be evaluated. In general, these measurements cannot be performed under steady-state conditions at high temperatures. In the present work, we used the pulsed-laser heating technique to evaluate the Si–As T_0 curve in the Si-rich region of the phase diagram.

2. EXPERIMENT

Si–As solid-solution layers epitaxially grown on top of $\langle 100 \rangle$-oriented silicon substrates were obtained by 120-keV As-ion implantation and pulse Nd laser annealing. Several samples were prepared with As substitutional concentration from 2 to 12.5 at% as determined by 2-MeV Rutherford backscattering (RBS) and channeling technique. The As concentration was constant over a depth of about 100 nm, with a long tail extending up to a depth of 200 or 300 nm due to diffusion in the liquid phase. Details on the preparation and characterization of similar samples have been reported elsewhere [8].

These solution cannot decompose on the nanosecond time scale since the maximum As diffusivity in solid Si is of the order of 10^{-11} cm$^2 \cdot$ s^{-1} and its average diffusion length in 1 ns would be a negligible fraction of one atomic displacement. Pulsed-laser-induced melting will, thus, occur congruently prior to decomposition.

The samples were irradiated by a single shot of a Q-switched, frequency-doubled, ruby laser (347-nm wavelength), with a 20-ns pulse duration and an energy density up to 0.7 J $\cdot$ cm^{-2} and with a 30-ns Nd laser (1064-nm wavelength).

3. AMORPHIZATION OF THE Si–As SOLUTION; Nd LASER IRRADIATION

Typical time-resolved reflectivity (TRR) curves are reported in Fig. 1. These reflectivity signals refer to samples with 11 at% As concentration irradiated with different energy density pulses. The signals obtained for irradiations between 0.2 and 0.3 J $\cdot$ cm^{-2} are shown as dashed lines. The intensity of the reflected He–Ne laser beam does not reach the value corresponding to the liquid reflectivity but progressively increases with increasing energy density of the laser pulse from 0.2 to 0.3 J $\cdot$ cm^{-2}; in this case the He–Ne laser probes a region where solid and liquid regions are present. The surface melting threshold E_{th} was assumed to be the energy density at which the midpoint value between the solid and the liquid

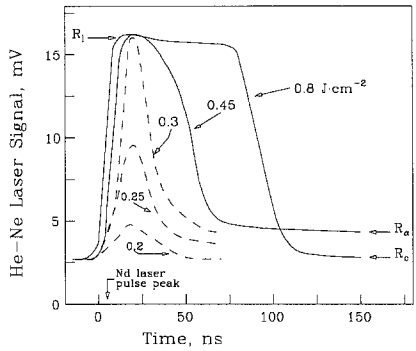

Fig. 1. TRR signals for ⟨100⟩-oriented Si with 11.1 at% As irradiated with 30-ns Nd laser pulses. Dashed lines: irradiations at energy densities near the melting threshold. Solid lines: irradiations at energy densities above the melting threshold.

reflectivity is reached by the signal of the reflected He–Ne laser beam. For this particular sample it is $E_{th} = 0.25\ J \cdot cm^{-2}$.

The solid lines refer to higher-energy density irradiation of 0.45 and $0.8\ J \cdot cm^{-2}$. The surface melt is well evidenced in this case by the plateau of the signal at the liquid reflectivity value. The reflectivity drops again to the value of the solid phase after 45 and 90 ns for the 0.45 and $0.8\ J \cdot cm^{-2}$ irradiation, respectively. However, the final levels are different. At the low-energy density irradiation it corresponds to the amorphous reflectivity, indicating that the liquid-to-amorphous transition took place. For higher-energy density ittadiation, instead, the final level is the same as the starting one, indicating that the crystal–liquid–crystal transition was induced by the laser pulse.

Transient reflectivity measurements were performed for several irradiation energy densities E and for different As concentration C_{As}. The results obtained by TRR measurements were confirmed by RBS analysis of the irradiated samples. In Fig. 2 the RBS spectra of the as-prepared sample with an As concentration of 11.1 at% and further irradiation with $0.45\ J \cdot cm^{-2}$ are reported. The solid line represents the random spectra of both samples; the irradiation with $0.45\ J \cdot cm^{-2}$ energy density, in fact, did not produce any further appreciable diffusion of As atoms compared with the diffusion induced by the adopted annealing procedure (three shots at $2\ J \cdot cm^{-2}$ for this sample). The 100-keV plateau extent in the As signal corresponds, in our glancing detection geometry, to a 75-nm-thick layer with 12.5 at% As concentration.

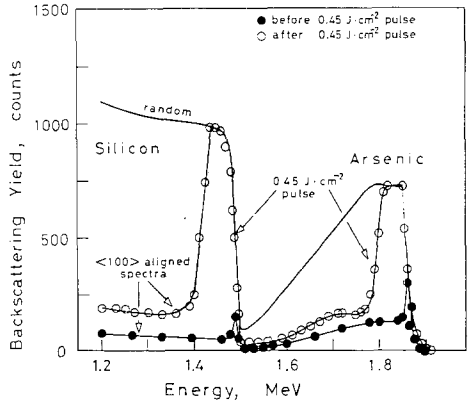

Fig. 2. 2-MeV He RBS spectra of crystalline Si–As alloy. Solid line: random spectrum. Filled circles: channeling along the ⟨100⟩ direction. Open circles: channeling along the ⟨100⟩ direction after irradiation with 30-ns Nd laser pulse at $0.45\ J \cdot cm^{-2}$.

The channeling spectrum for the starting sample is shown as filled circles. The minimum yield in the silicon signal is about 4%, indicating a good crystal quality. The minimum yield in the arsenic signal is 13%, indicating that the substitutional concentration is 11.1 at%; this means that not all the arsenic atoms are ini a lattice site but rather in interstitial position. In all the samples, the substitutional concentration was slightly lower than the total concentration. Throughout the entire paper, we neglect the contribution of the interstitial atoms.

The aligned spectrum for the 0.45 $J \cdot cm^{-2}$-irradiated sample is shown as open circles. An amorphous layer 50 nm thick is evident from both the Si and the As signals. The presence of the amorphous phase was checked by electron diffraction analysis.

The measured energy densities of the laser pulse to induce the liquid to amorphous transition are correlated with the regrowth velocity. Moreover, knowing the As concentration for each sample, it is possible to correlate this last quantity with the critical solidification velocity. The results are plotted in Fig. 3a for both the $\langle 111 \rangle$ (circles) and the $\langle 100 \rangle$ (squares) orientations. The experimental points of pure silicon are also reported. For the same As concentration, the critical amorphization

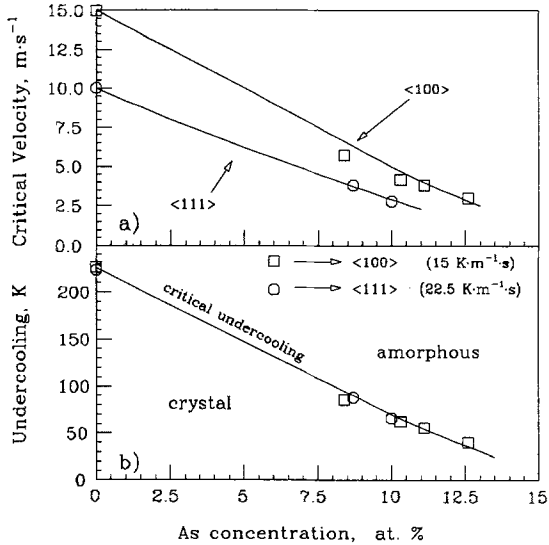

Fig. 3. (a) Critical solidification velocity to nucleate the amorphous phase for a Si–As alloy as function of As concentration for $\langle 100 \rangle$ and $\langle 111 \rangle$ substrates. (b) Critical undercooling of the Si–As liquid solution to nucleate the amorphous phase.

velocity is lower for the ⟨111⟩ substrates than for the ⟨100⟩ ones as for pure silicon.

The velocity–undercooling relationship can be used to convert the abscissa scale into a temperature scale. The undercooling for liquid-epitaxial regrowth along the ⟨100⟩ direction in Si is $15\ \mathrm{K \cdot m^{-1} \cdot s}$ [9] and molecular-dynamics computations [9, 10] allow us to extend this result to the ⟨111⟩ direction of growth by scaling with a factor 1.5. We thus assumed $22.5\ \mathrm{K \cdot m^{-1} \cdot s}$ undercooling for the liquid phase epitaxy along the ⟨111⟩ direction. The liquid temperature associated with the two different critical velocities for the ⟨111⟩- and ⟨100⟩-oriented pure Si samples are then the same.

By replotting the ⟨100⟩ and ⟨111⟩ data in Fig. 3a in terms of amount of undercooling through its relationship with the velocity, a single curve has been obtained as shown in Fig. 3b.

The solid line labeled "critical undercooling" separates two regions: in the upper region solidification will result in an amorphous layer, while in the lower one full epitaxial regrowth will take place. It is also possible to extrapolate toward a critical value of As concentration (about 15 at%) at which no undercooling of the liquid below its equilibrium temperature with the crystalline solid is needed to solidify the amorphous phase.

The experimental results demonstrate that the pulsed laser-induced amorphization of a supersaturated crystalline Si–As solution in the 7–13 at% As concentration range exhibits the same qualitative features as pure silicon. The transition to the amorphous phase takes place via liquid phase when the solidification velocity exceeds a critical value which depends on the substrate orientation.

A strong correlation between the As concentration and the critical velocity has also been found. All our data are consistent with the hypothesis that the difference between the crystal and the amorphous melting points decreases with increasing As concentration. This temperature difference is in turn the minimum amount of undercooling with respect to the crystal–liquid equilibrium temperature needed to nucleate the amorphous phase from the liquid. At the moving solid–liquid interface, the undercooling is driven by the solidification velocity; thus the critical velocity will decrease with increasing As concentration.

To make this explanation plausible one assumption has been made, that is, that the velocity response functions for the Si–As solution and for pure Si are the same. In order to justify this assumption, pulsed laser irradiation has been employed to measure the T_0 curve of the Si–As system.

4. MELTING OF Si–As SUPERSATURATED SOLUTION; UV IRRADIATION

In Fig. 4 the peak value of the argon-laser reflected light signal is reported as a function of the UV irradiation energy density for samples with 2, 8, and 12.5 at% As concentration and for pure Si. In this last case the plateau was detected only at energy densities above $0.6\ J \cdot cm^{-2}$, with a liquid reflectivity signal of 22.5 mV and time extension of the plateau greater than 15 ns. The small increase in the signal (from 1 to 4 mV) for irradiation energy densities between 0 and $0.4\ J \cdot cm^{-2}$ is consistent with surface heating.

In the 0.4–$0.6\ J \cdot cm^{-2}$ irradiation energy density range, a Gaussian-shaped signal with a full width at half-maximum (FWHM) of about 15 ns and a peak value between that of the hot solid and that of the liquid was observed. A mixture of solid and liquid phases is probed by the argon-laser beam in this case, and the correct melting threshold (i.e., the irradiation energy density E_{th} for which the surface temperature reaches the melting point) lies in this range.

For the Si–As samples the behavior of the signal is similar to that of pure Si with the minor difference that the solid reflectivity increases with As concentration, while that of the liquid decreases. The major difference is the shift of all the signals toward lower energy densities with increasing As content.

Modeling the surface melting by heat flow calculations [11] yields an almost-linear relationship between the energy density of the laser pulse and

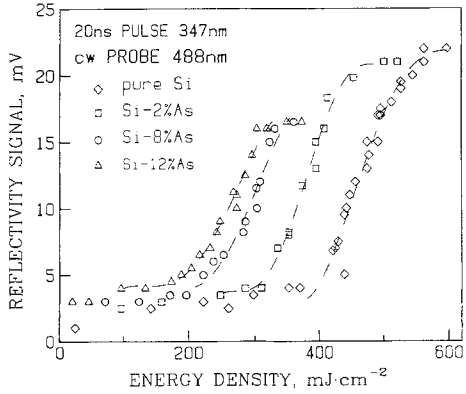

Fig. 4. Reflectivity peak signal for a 488-nm Cw probe as a function of fluence for Si samples with different As concentrations, irradiated with 20-ns 347-nm laser pulses.

the maximum surface temperature. Based on this trend, the melting thresholds can be concerted into temperature, knowing the melting temperature of pure Si.

The adopted heat flow model, however, does not account for any dependence of the thermal parameters on the As concentration, and the values for pure Si are used for all the samples. The evaluated melting temperature may be incorrect; if the thermal diffusivity of the As alloyed layers decreases with increasing As concentration, then their melting threshold energy density would be reduced as well, even for the same melting temperature.

To remove this uncertainty on the true case of the observed melting-point reductions, we reperformed the experiment for one sample with 10 at% As concentration, employing laser pulses of different pulse duration and wavelength, 20 ps and 532 nm, respectively.

The valuated melting points of the nanosecond experiment are shown in Fig. 5 (open squares) together with that evaluated by the picosecond experiment (filled square). A solid line interpolates experimental data. The reported error bars for the data of the UV experiment were estimated from the statistical dispersion of the melting threshold energy densities measured for several samples with the same As concentration. These experimentally determined melting points represent the so-called T_0 curve of the Si–As system.

In a similar way, we measured the T_0 curve of the amorphous solution. We amorphized the same crystalline samples used before by means of ion implantation of As^+ ions in order to have surface amorphous

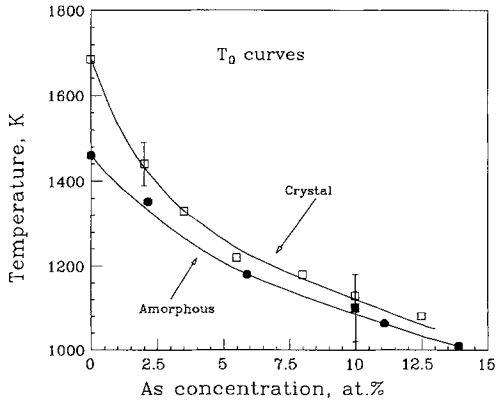

Fig. 5. Melting points of the crystalline (open and filled squares) and amorphous (filled circles) solutions as a function of As concentration.

layers of thickness greater than the absorption length of the UV light in amorphous Si. Measurements of the optical constants (not shown here) of the amorphous Si–As solutions did not show any appreciable variation with As content. The results shown in Fig. 5 (filled circles) clearly indicate a reduction of the melting point with As concentration but in a smoother way than for the crystalline solution; then the difference of the melting points of the crystalline and amorphous solutions decreases with increasing As concentration. This confirms what we found in the case of the Nd laser irradiations shown above.

Some other informations can be extracted from the T_0 curve of the crystalline alloy. In Fig. 6, the Si-rich part of the Si–As phase diagram is shown together with the T_0 curve. Solid lines in the figure are the solidus and liquidus curves of the assessed Si–As phase diagram [12]. In the high-temperature region (above 1300 K), the T_0 curve lies inside the region of the stable solid delimited by the solidus line adopted from Refs. 13 and 14. This is a nonphysical result.

It is well known, however, that upon thermal treatment of laser-annealed Si–As solid solutions, the electrically active As atoms are only a minor fraction of the substitutional ones [15]. The electrically active solute concentration has been shown to depend on the temperature only [16, 17]. Some available solubility data determined by electrical measurements [16–18] are reported as small open symbols in Fig. 6. Recently, it has been

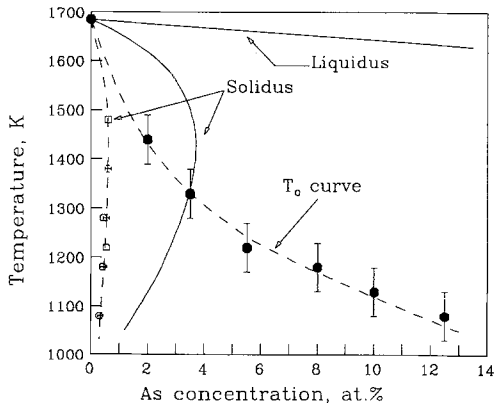

Fig. 6. Large filled circles: melting point vs As concentration of Si–As solid solutions, nanosecond experiment. Small open symbols: solid solubility data from Refs. 16, 17, and 18. Solid lines: solidus and liquidus curves of the assessed Si–As phase diagram. Dashed line: polynomial interpolation of the experimental data.

shown that the electrically active As concentration coincides with the solubility, since the electrically inactive part is a precipitate phase although apparently in a substitutional Si lattice site [19]. The solubility data from electrical measurements are then more likely to give the true solidus line of the phase diagram. Our result is consistent with only this second solidus curve.

5. CONCLUSIONS

In this work, we show the capability of laser irradiation to provide information on the thermodynamic properties of solids. By means of extremely rapid heating and quenching rates, it allows the study of metastable phases in a temperature range otherwise not allowed.

In particular, we investigated the properties of the crystalline and amorphous Si–As system. We found a direct evidence of the lowering of the metastable melting points of both the crystalline and the emorphous solutions as the arsenic concentration is increased. For the crystalline solution, however, the decrease is steeper; this leads to a progressive reduction of the difference between the two melting points. Extrapolating this result to higher As concentration it seems that a concentration should exist at which, however slow the process of solidification, the amorphous phase will be quenched. Moreover, on comparing the measured T_0 curve with the solidus line of the assessed Si–As phase diagram, we found the former in agreement only with the solidus line determined by means of electrical measurements, supporting the hypothesis of the presence of some form of clustering of the arsenic atoms.

REFERENCES

1. See, for example, as a review paper, P. S. Peercy, M. O. Thompson, and J. Y. Tsao, in *Beam Solid Interaction and Transient Process*, Material Research Society Symposium Proceedings, Vol. 74, M. O. Thompson and J. S. Williams, eds. (MRS, Pittsburgh, 1987), p. 15.
2. J. M. Poate, *Nucl. Instrum. Methods* **209–210**:211 (1983).
3. P. Baeri, G. Foti, J. M. Poate, and A. G. Cullis, *Phys. Rev. Lett.* **45**:2036 (1980).
4. A. G. Cullis, H. C. Webber, N. G. Chew, J. M. Poate, and P. Baeri, *Phys. Rev. Lett.* **49**:219 (1982).
5. M. von Allmen and S. S. Lau, in *Laser Annealing of Semiconductors*, J. M. Poate and J. M. Mayer, eds. (Academic, New York, 1982), p. 439.
6. M. O. Thompson, G. J. Galvin, J. W. Mayer, P. S. Peercy, J. M. Poate, D. C. Hacobson, A. G. Cullis, and N. G. Chew, *Phys. Rev. Lett.* **52**:2630 (1984).
7. J. A. Knapp and D. M. Follstaed, *Phys. Rev. Lett.* **58**:2454 (1987).
8. P. Baeri and R. Reitano, *Phys. Rev.* **B**39:13231 (1989).
9. G. H. Gilmer, *Mat. Sci. Eng.* **65**:15 (1984).

10. J. Q. Broughton, G. H. Gilmer, and K. A. Jackson, *Phys. Rev. Lett.* **49**:1496 (1982).
11. P. Baeri and S. U. Campisano, in *Laser Annealing of Semiconductors*, J. W. Mayer and J. M. Poate, eds. (Academic, New York, 1982), p. 75.
12. R. W. Olesinski and G. J. Abbaschian, *Bull. Alloy Phase Diagram* **6**:254 (1985).
13. F. A. Trumbore, *Bell Sysxt. Tech. J.* **39**:205 (1960).
14. J. S. Sandhu and J. L. Reuter, *IBM J. Res. Dev.* **15**:464 (1971).
15. A. Leietola, J. F. Gibson, T. J. Magee, J. Peng, and J. D. Hong, *Appl. Phys. Lett.* **35**:532 (1979).
16. A. Leietola, J. F. Gibson, and T. W. Sigmon, *Appl. Phys. Lett.* **36**:765 (1980).
17. D. Nobili, A. Carabelas, G. Celotti, and S. Solmi, *J. Electrochem. Soc.* **130**:922 (1983).
18. N. Miyamoto, E. Kuroda, and S. Yoshida, *J. Jpn. Soc. Appl. Phys. Suppl.* **43**:408 (1974).
19. A. Armigliato, D. Nobili, S. Solmi, A. Bourut, and P. Werner, *J. Electrochem. Soc.* **133**:2560 (1986).